OPTIMAL DESIGN OF CERAMIC/SANDWICH COMPOSITE STRUCTURES TO BETTER RESIST FOR AP PROJECTILE IMPACT

Serei B. Sapozhnikov[1], Galina A. Forental[1]

[1]South Ural State University, Physics Department, 76, Lenin ave., Chelyabinsk, 454080, Russia
Email: sapozhnikovsb@susu.ru, Web Page: http://zief.susu.ru

Keywords: high velocity impact, FEA fracture models, ceramics, sandwich composite optimal design

Abstract
The typical ceramic/composite personal protective structures now are monolithic. In this case, alumina ceramic part is designed to shatter high hardness core of projectile into fragments and AFRP part's role is full dissipation of residual energy of these fragments. For alumina ceramic we proposed low-parametric pseudo-brittle failure model which is identified by simple quasi-static tests (ring-on-ring bending) and high hardness steel sphere ballistic tests (using table-top gunpowder stand). We assumed that 'pseudo-brittle' term means: compression behaviors of ceramics are elastoplastic but tension ones - pure elastic up to failure. Failure model of layered composite is fibre-oriented, so only fibre's fracture plays main role on energy dissipation during penetration. Thus, pure elastic and brittle dynamic fracture in fibres direction is actual. All other directions behaviors (all shears and transversal) are unlimitedly elastic. Thus, among nine orthotropic strength parameters only two (tension and compression in fibre directions) are valuable. For numerical estimation of ballistic curves, we used ANSYS AUTODYN-3D® explicit code with 'death of elements' approach and remaining of eroded element's inertia. Splitting composite part into two different thickness pieces we have designed optimal sandwich structure which has 20% less weight with the same AP resistance as of monolithic one.

1. Introduction

Modern ceramics/FRP protective structures are widely used to defeat armor piercing (AP) bullets due to low areal density, high face hardness, and the ability to dissipate the bullet and ceramic fragments energy by fibre's fracture and delamination [1]. The best compositions nowadays consist of boron or silicon carbide face layer and UHMWPE backing plate [2, 3]. Areal weight is about 30-35kg/m2 (Level III, STANAG 4549, 7.62 AP B-32 bullet, 840 m/s). These projects are used for personal protection [3, 4] where minimum weight is mostly demanded. Otherwise, for the ground vehicle armor there are frequently used combinations of alumina/aramid fibre reinforced plastic (AFRP) backing plate [5]. At the same loading conditions (Level III, STANAG), areal density of this combination is about 50-52 kg/m2. A Monolithic alumina plate is good to withstand only one shot, because multiple radial cracks after first impact decrease the reliability of that protective structure for next impacts [6, 7]. Pelletizing of alumina block is a modern way to construct multi-hit protection [8], but weight goes up by 10-15% because of weak zones near the borders of ceramic tiles/pellets. In this case, we need to save weight from composite backing part by using, for example, sandwich structure instead of monolithic one. Very close analogy could be taken from space hypervelocity impact protection (Whipple shields with aluminium and Nextel-Kevlar bumper layers [9]): an external, thin bumper shield that is exposed to the debris flux and causes the impactors to completely disintegrate during impact. The resulting cloud of projectile debris and bumper material that is formed behind the bumper leads to a much wider spatial distribution of momentum, allowing the back face of the shield to withstand the impact pressure.

Excerpt from ISBN 978-3-00-053387-7

The current study investigates and demonstrates the relationships between residual velocity of AP projectile after penetration of ceramics/composite target and dimensional parameters of this target. Experimental data to validate numerical models of ceramics and FRPs are described. Effect of sandwich skin thickness' ratio on the overall armor ballistic performance will then be presented, following the numerical model and simulation results.

2. Experimental

2.1. Modelling materials

To understand the basics of alumina/AFRP target penetration with high hardness AP projectile we have chosen firstly the commercially available modelling materials: 4.84 mm of thickness soda-lime glass (as 'ceramic layer'), 2 mm of thickness GFRP 'STEF' (as 'AFRP laminate' with close mechanical behaviours) and 6.35 mm of diameter tempered steel ball (as 'AP projectile' with close to high hardness core mechanical behaviours).
Using static and different dynamic conditions the modelling materials were tested in the following way:
1. Weighing to define density;
2. Tension of GFRP coupons in warp, weft and diagonal directions to estimate elastic modules and strength using quasi-static testing machine INSTRON 5882;
3. Ring-on-ring bending test to determine the tensile strength of glass;
4. High velocity impact tests of materials using steel ball to get ballistic curves.
All data of 1-3 items are collected in Table 1. In brackets, there are fitted dynamic strength data for glass and GFRP after ballistic penetration and numerical calculations.

Table 1. Mechanical behaviors of materials.

Material Type	Density, (g/cm^3)	Modulus of elasticity (GPa)	Poisson's ratio	Strength (MPa)
Soda-lime glass	2.50	73	0.20	σ_u =100 (200)
Tempered high carbon steel [10]	7.85	210	0.30	σ_{yield}=1300 σ_u=1800 $E^{tangent}$=13000
GFRP 'STEF', x – warp, y - weft	2.00	$E_x=E_y=27.0$, $E_z=8.0$, $G_{xy}=4.0$, $G_{xz}=G_{yz}=3.5$	ν_{xy}= 0.15, ν_{xz}= 0.40, ν_{yz}= 0.40	$\sigma_{u\,x}=\sigma_{u\,y}$ = 400 (900)

The ballistic tests were performed using the 6.35 mm of diameter tempered steel ball accelerated (with 0.2g polyethylene disk-shaped sabot) up to 900 m/s by means of energy of standard dowel cartridge on special lab-scale stand [11], Fig. 1.
Initial bullet velocity V_i was measured by the optical chronograph and residual velocity V_r (after penetration of target) was measured by special frictional trap. Trap sliding distance S along rail at dry friction conditions vs V_r was calibrated by ball shots without target. All ballistic experiments' data were collected as V_r vs V_i graphs (ballistic curves) and then least-squares fitted by use of classical Lambert-Jonas [12] formula:

Excerpt from ISBN 978-3-00-053387-7

$$V_r = \begin{cases} 0 \; if \; V_i < V_L \\ A \cdot \left(V_i^k - V_L^k\right)^{1/k} if \; V_i \geq V_L \end{cases}, \tag{1}$$

where V_L is ballistic limit, A and k – regression parameters.

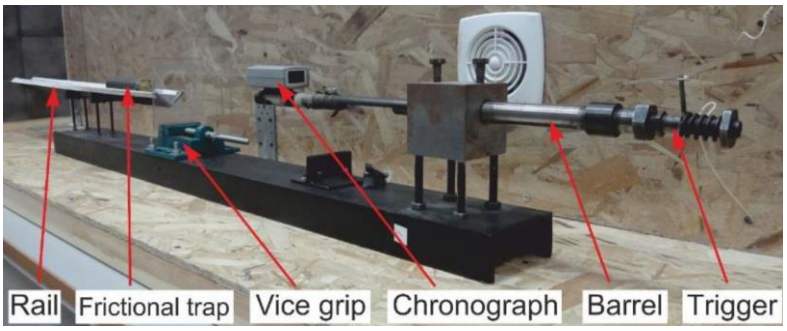

Figure 1. Lab-scale gunpowder stand.

2.2. Numerical modelling

In this part, we are considering the methodological problems to work with brittle materials like glass or ceramics and composites. In literature, we can find out different failure models, but most popular among them are Johnson-Cook and Johnson-Holmquist failure models of ductile or brittle materials. Johnson and Holmquist model [13, 14] has up to 20 parameters, which are to be determined before calculations. However, using custom materials users faced a difficult choice to find known material close to user one and then to use known data in calculations or to try the use simpler model with much lesser number of parameters. To speak in favour of using the second way we can offer some reasons. Impact velocities are in the range of 100-900 m/s, when the compressibility of dense solids (glass, GFRP, ceramics) is not so high, strain rate varies in one order. This can lead us to use all mechanical characteristics insensitive of strain rate in calculations. Quasi-static values of strength characteristics should be increased (typically in 2-2.5 times) to fit the experimental data on ballistic impact. Therefore, we can consider ceramics in described conditions as isotropic incompressible elastic-plastic medium and construct its stress-strain law with failure when the first principal stress reaches the corresponding tensile strength σ_u, Figure 2a.

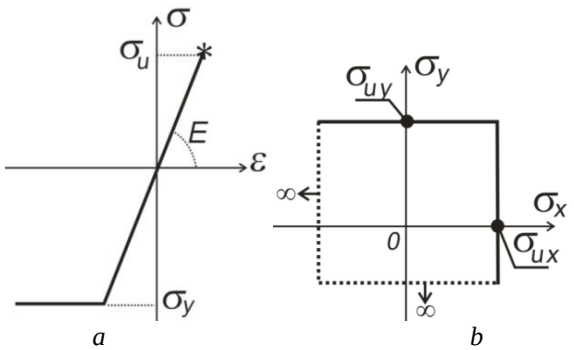

Figure 2. Failure models of ceramics (a) and GFRP (b).

This simple model reflects the most valuable feature of ceramics: brittleness at tension and pseudo-ductility at compression. We can say that ductility of ceramics now is very popular item especially at indentation (local compression) [15-17]. There are no visible cracks in our model and only 'death of finite elements' (with remaining inertia) is in FE formulation.

Excerpt from ISBN 978-3-00-053387-7

For GFRP the model of material is orthotropic elastic. Failure is stress driven process along warp and weft directions achieving corresponding tensile strength. This is assumed because fibers in FRP are the strongest and most energy consuming parts. Matrix stiffness is very low and energy of fracture is low, too. So, we consider that all shear and transversal compressive strength can be taken as an infinite one (1*1020 during calculations), Figure 2b.
Layered GFRP can also be damaged during transversal tension leading to delamination. In our protective structures all bonded contacts were modeled as breakable (tensile and shear strength are 100 MPa) to get realistic value of delamination area. Material of tempered steel ball was assumed to be elastic-plastic.
ANSYS/AUTODYN explicit code offers to erode FE from the mesh if its distortion became great (Geometric Strain Limit > 1). This approach helps to prevent the drastic reduction of time step.
Next factor is the size of FE mesh at the modelling. To predict FE failure, explicit code like ANSYS/AUTODYN or LS-DYNA uses FE with one integration point. Therefore, the gradient of stress or strain at failure of FE is not considered [18]. This is obviously the indirect mechanism to include the toughness of material in numerical modelling (toughness is the instrument to measure of material's sensitivity to stress/strain gradient). Smaller size of FE – lesser toughness of the material.
Preliminary impact calculations in the range closed to ballistic limit showed that the rational size of FE mesh of glass, alumina and FRP had to be ~1…2 mm. Experimental and numerical results of penetration of glass plate, GFRP and combination of glass/GFRP are depicted in Figure 3. Tested plates were vice-gripped by one side. Pictures of penetrated plates are shown in Figure 4.

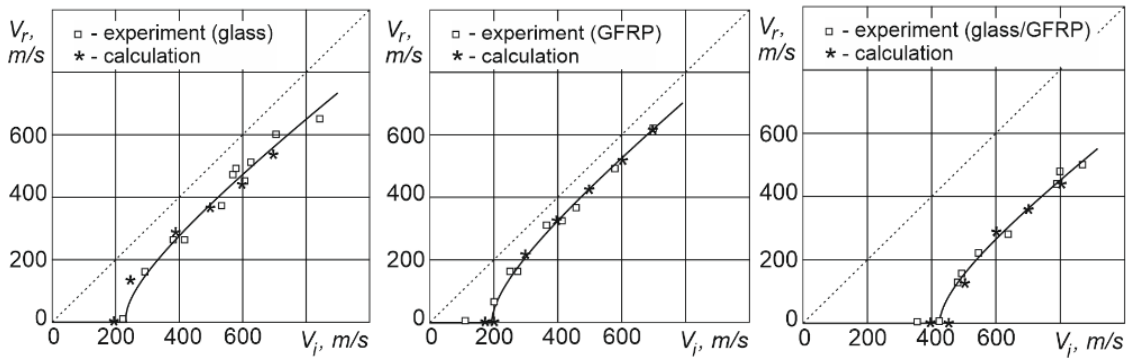

a *b* *c*

Figure 3. Ballistic curves for targets: glass (a), GFRP (b) and glass/GFRP combination (c). Lines – fit of experimental data by Lambert-Jonas eq. (1).

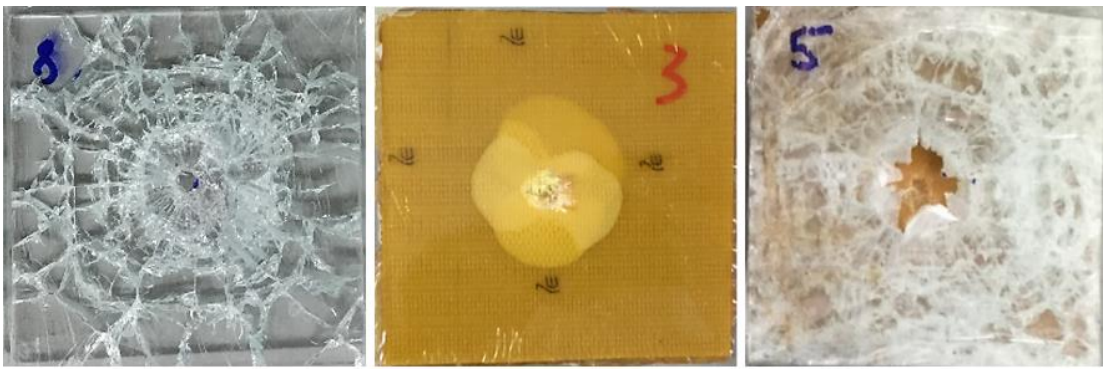

a *b* *c*

Figure 4. Samples (100x100 mm) of glass (a), GFRP (b) and glass/GFRP composition (c).

Very good comparison of ballistic tests and numerical results for penetration of glass, GFRP and layered glass/GFRP structure gave us the possibility to estimate the ballistic performance of alumina/AFRP composite using the same simple 'pseudo-brittle' low-parametric approach.

Excerpt from ISBN 978-3-00-053387-7

3. Ballistic performance of alumina/AFRP composite

3.1. Monolithic targets

It is known that combination of 10 mm of alumina thickness and 10 mm of thickness AFRP block can defeat the threat level III of STANAG 4849 with 7.62x54 AP B-32 (840 m/s) projectile [19]. AP B-32 projectile consists of high hardness steel core (~68HRC), and low-carbon steel jacket, Figure 5. Jacket was modelled by elastic-plastic steel with yield stress σ_y=150 MPa, core was pseudo-brittle steel with σ_y=1300 MPa, σ_u=1800 MPa. 60% of the bullet core length was designed to be eroded and back 40% was elastic-plastic and non-fractured. This reflects the experimental observations with tempered steel cores after penetration of ceramics/composite tiles. Alumina was pseudo-brittle (elastic-plastic) isotropic media with σ_y=σ_u=1350 MPa, E=390 GPa, ν=0.22. AFRP was modelled by orthotropic media with E_x=E_y=40 GPa, E_z= 8 GPa, G_{xy}= 3 GPa, G_{xz}= G_{yz}= 2 GPa, ν_{xy}= 0.14, ν_{xz}= 0.3, ν_{yz}= 0.3, σ_{ux} = σ_{uy} = 1000 MPa, σ_{uz}= 100 MPa. The size of FE mesh for ceramics, AFRP and bullet was in a range of 1…2 mm.

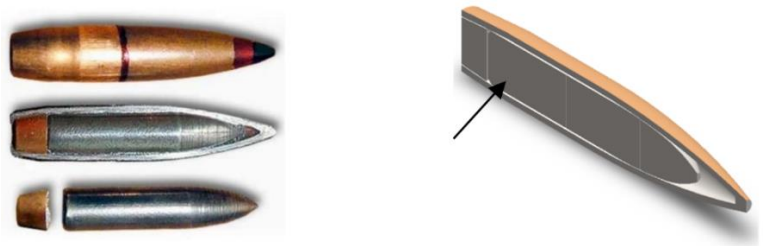

Figure 5. The components of the 7.62x54 AP (B-32) bullet, left: full view, steel jacket, high hardness steel core and ignition cup; right: 3D model of bullet (section), arrow shows elastic part of the core.

3.2. Sandwich targets

Here we designed ceramics/sandwich composite system (for the same Level III of STANAG) with using 10 mm of alumina thickness and t1, t2 – thickness of the outer and inner skin of sandwich AFRP panel. Total thickness of protective system was restricted by 30 mm to adopt for shielding application. In this case, 20 mm of total thickness was occupied by sandwich structure. Influence of the foam core of sandwich on ballistic resistance was excluded.
We investigated several projects of sandwiches where t1=0…10 mm and t2= 0…10 mm. 2D graph of penetration results is shown in Table 2 (x – penetration, o – absence of penetration). Best projects are highlighted (4/4 and 2/6). In these cases, weight of sandwich backing is 20% less than of monolithic one (10/0). For future application second variant (2/6) is better because area of delaminating in outer skin (t1=2 mm) is smaller and this is good for reliability in case of use of discrete ceramic elements (tiles) to increase of protection structure's reliability.

Table 2: Penetration results.

		t_1, mm					
		0	2	4	6	8	10
t_2, mm	10	x	o	o	o	o	o
	8	x	o	o	o	o	o
	6	x	**o**	o	o	o	o
	4	x	x	**o**	o	o	o
	2	x	x	x	x	o	o
	0	x	x	x	x	x	o

Excerpt from ISBN 978-3-00-053387-7

Cross-sections of successful/unsuccessful projects are depicted in Figure 6 (*a*, *b*) and 7 (*a*-*f*). Pictures *a*-*c* show the absence of penetration. Pictures d-f – full penetration. Figure 8 shows the deceleration of B-32 AP bullet during the penetration of the above targets.

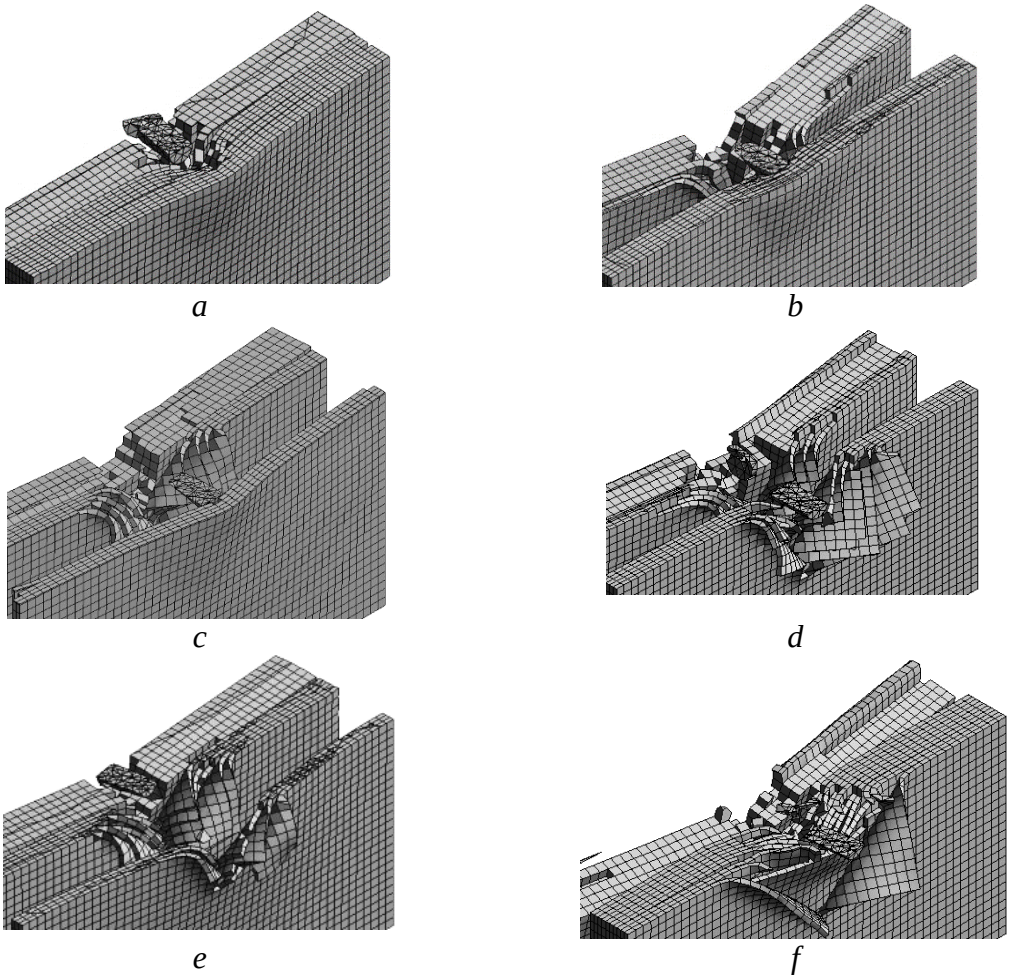

Figure 6. Pictures of penetration, projects: t1/t2=10/0 (*a*), 2/6 (*b*), 4/4(*c*), 3/5(*d*), 5/3(*e*), 0/10(*f*) for the period of time 0.00025 s.

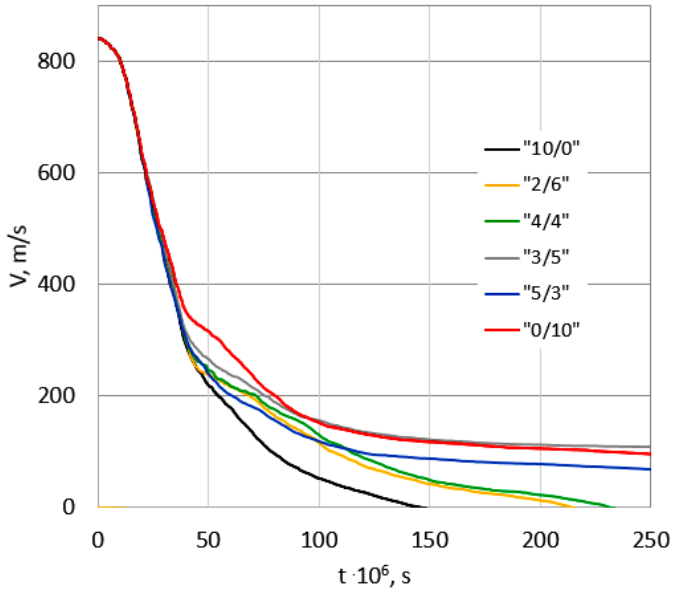

Figure 7. Deceleration of B-32 projectile (velocity vs time) during the contact of different projects.

Excerpt from ISBN 978-3-00-053387-7

4. Results and discussions

In the design of ballistic protection structures with explicit simulations, the success of numerical models highly depends on several features. First, the material descriptions should be modelled accurately to exhibit realistic behavior during penetration. For glass and alumina these features are local plasticity at compression contact and brittle fracture at tension. For FRPs, there are complexities of fracture mechanisms because of significant anisotropy of these materials. In this work, we proposed numerically effective, low-parametric and adequate models of ceramics and FRPs to predict ballistic performance of ceramics/FRP protective structures.
The most informative thing is ballistic curve getting after dozen experiments with perforation of targets with different projectile velocities. The numerical prediction of ballistic limit V_L is highly dependent on compressive plasticity of ceramics and size of finite element. Therefore, these values can easily be tuned to get proper dynamic behavior of material by fitting ballistic experiments' data on separate ceramics tiles. For higher velocities the influence of material's inertia (density) becomes clear and strength plays secondary role. To describe failure model of ceramics we need to have only two parameters: compressive yield stress and tensile strength (to be increased from static value up to 2…2.5 times). For failure model of FRPs (GFRP and AFRP) we offer to use again two parameters: dynamic tensile strength along fibres (or along warp and weft - for fabrics) and transversal tensile strength (as breakable bonded contacts between layers). For fabric-reinforced plastics, the dynamic strength along fibres' direction is 2…2.5 times higher than the static one. All other strength characteristics are not so valuable for ballistic performance. We have checked these very simple models on soda-lime glass, GFRP separately and with combination of glass/GFRP panels under steel ball ballistic loading. Comparison of experimental and numerically given ballistic curves showed very good results for engineering applications.

5. Conclusions

In this study, the penetration resistance of hard face composite structures (alumina/AFRP) against 7.62x54 AP bullet has been determined numerically on the base of experimental and numerical modelling of impact of high hardness 6.35 mm steel ball on soda-lime glass (as alumina analogue), GFRP plate (as AFRP analogue) and laminate glass/GFRP. The numerical models were developed using Lagrange discretization to simulate fragmentation ('death of elements' technique with remain of inertia) and complex penetration behaviors of targets. According to numerical and experimental data developed during the study, the following main conclusions can be drawn: it is possible to use only two dynamic failure parameters of ceramics and two dynamic parameters of composite backing to predict the results of ballistic impact. These models of materials gave us the possibility to optimize novel protective structure consisting of ceramic face and sandwich backing. The weight of optimised sandwich part is 20% less than that of a monolithic one with the same ballistic performance.

Acknowledgments

This work was carried out in South Ural State University (National Research University) with a financial support of Russian Science Foundation (project № 14-19-00327). The authors thank Dr. Sergei G. Ivanov (Oklahoma, USA) for the fruitful discussions.

References

[1] Hazell P.J. Ceramic Armor: Design and Defeat Mechanisms, Canberra, Argos Press: Canberra, pp.168, 2006.

[2] Ong, C.W., Boey, C.W., Hixson, R.S. and Sinibaldi, J.O. Advanced layered personnel armor. International Journal of Impact Engineering, 38, pp. 369-383. 2011.

Excerpt from ISBN 978-3-00-053387-7

[3] Bürger, D., de Faria, A.R., de Almeida, S.F.M., de Melo, F.C.L., Donadon, M.V. Ballistic impact simulation of an armor-piercing projectile on hybrid ceramic/fiber reinforced composite armors. International Journal of Impact Engineering, 43, pp. 63-77, 2012.

[4] Holmquist, T.J., Johnson, G.R. Response of boron carbide subjected to high-velocity impact. International Journal of Impact Engineering, 35, pp. 742-752, 2008.

[5] Danzer, R. On the relationship between ceramic strength and the requirements for mechanical design. Journal of the European Ceramic Society, 34(15), pp. 3435-3460, 2014.

[6] Levy, S., Molinari, J.F. Dynamic fragmentation of ceramics, signature of defects and scaling of fragment sizes. Journal of the Mechanics and Physics of Solids, 58, pp. 12-26, 2010.

[7] Lee, M., Kim, E.Y., Yoo, Y.H. Simulation of high-speed impact into ceramic composite systems using cohesive-law fracture model. International Journal of Impact Engineering, 35, pp. 1636-1641, 2008.

[8] Clayton, J.D. Penetration resistance of armor ceramics: Dimensional analysis and property correlations. International Journal of Impact Engineering, 85, pp. 124-131, 2015.

[9] ESA, http://www.esa.int/Our_Activities/Operations/Space_Debris/Hypervelocity_impacts_and_protecting _spacecraft.

[10] Kilic, N., Ekici, B. Ballistic resistance of high hardness armor steels against 7.62 mm armor piercing ammunition. Materials and Design, 44, pp. 35-48, 2013.

[11] Sapozhnikov, S.B., Kudryavtsev, O.A., Dolganina, N.Y. Experimental and numerical estimation of strength and fragmentation of different porosity alumina ceramics. Materials and Design, 88, pp.1042-1048.

[12] Zukas, J.A., Nicholas, T., Swift, H.F., Greszczuk, L.B., Curan, D.R. Impact dynamics. New York: J. Wiley, pp. 332, 1982.

[13] Johnson, G.R., Holmquist, T.J. A computational constitutive model for brittle materials subjected to large strains, high strain rates, and high pressures. Proc. of EXPLOMET Conference (San Diego, California). New York: Marcel Dekker Inc., pp. 1075-1081, 1992.

[14] Johnson, G.R. Numerical algorithms and material models for high-velocity impact computations. International Journal of Impact Engineering, 38, pp. 456-472, 2011.

[15] Deshpande, V.S., Evans, A.G. Inelastic deformation and energy dissipation in ceramics: A mechanism-based constitutive model. Journal of the Mechanics and Physics of Solids, 56, pp. 3077-3100, 2008.

[16] Clayton, J.D., Kraft, R.H., Leavy, R.B. Mesoscale modeling of nonlinear elasticity and fracture in ceramic polycrystals under dynamic shear and compression. International Journal of Solids and Structures, 49, pp. 2686-2702, 2012.

[17] Wereszczak, A.A., Morrisey, T.G., Ferber, M.R., Bortle, K.P., Rodgers, E.A., Tsoi, G., Montgomery, G.M., Vohra, Y. and Toller, S. Responses of siliceous materials to high pressure. Advances in ceramic armor IX, Ceramic engineering and science proceedings, 34(5), p.1-14. 2013.

[18] ANSYS ® Help, v.16.0, SAS IP Inc., 2014.

[19] Ogorkiewicz, R.M. Armor for light combat vehicles. Int. Defense Review, 35, July, p.41-45, 2002.

Excerpt from ISBN 978-3-00-053387-7